Journal of ELECTRONIC MATERIALS, Vol. 48, No. 9, 2019
https://doi.org/10.1007/s11664-019-07386-1

Effects of Electrical Properties on Determining Materials for Power Generation Enhancement in TEG Modules

TURGUT OZTURK ,[1,6] ENES KILINC,[2] FATIH UYSAL,[2] ERDAL CELIK,[3,4] and HUSEYIN KURT[5]

1.—Department of Electrical-Electronics Engineering, Bursa Technical University, Bursa, Turkey. 2.—Department of Mechanical Engineering, Faculty of Engineering, Karabuk University, Karabuk, Turkey. 3.—Council of Higher Education, Bilkent, Ankara, Turkey. 4.—Department of Metallurgical and Materials Engineering, Faculty of Engineering, Dokuz Eylul University, Izmir, Turkey. 5.—Department of Mechanical Engineering, Faculty of Engineering and Architecture, Necmettin Erbakan University, Konya, Turkey. 6.—e-mail: turgut.ozturk@btu.edu.tr

This study aimed to increase the energy efficiency of thermoelectric generators designed by considering the electrical properties of *p*- and *n*-type semiconductor materials for reducing the costs associated with the experiments, errors, and long production processes. Accordingly, the estimation of the energy amount to be produced by the thermoelectric materials was achieved by different doping elements using three different parameters such as skin-depth, electrical conductivity and dielectric constant. Additionally, the findings were supported by experimental results. In contrast to the conventionally used black-box type approach and estimation methods, an inference was obtained on the actual values of the materials.

Key words: Conductivity, permittivity, skin-depth, k-means, thermoelectric materials, power generation, rare-earth elements

INTRODUCTION

Over the globe, 80% of total heat energy is produced by power plants consuming fossil fuels, and 26% of it is wasted into the atmosphere.[1,2] Thus, fuels must be converted into energy by clean methods. Additionally, there is a secondary energy source in waste energy that must be recovered in efficient, sustainable and clean ways.[3] With the increasing demand for clean energy, the interest of researchers in alternative energy resources has increased.[4] Thermoelectric generators (TEGs), which are quiet, compact and have no maintenance requirements, may be used to recover waste heat energy.[5,6] Therefore, thermoelectric materials (TEMs) have been used to convert heat energy into electrical energy directly, and they have become a focus of interest for many researchers. By producing heat-resistant TEMs, high-efficiency TEGs may be designed. However, expensive production and testing stages and respectively lower efficiency levels of TEGs indicate a need for alternative solutions.[6–8] For this purpose, before design and production processes, prediction of electrical properties of the semiconductor materials in TEGs will be useful in determining which semiconductor materials are more suitable to reach higher efficiency levels under specific operating conditions. Therefore, electrical conductivity and permittivity parameters of semiconductors at high temperatures may be utilized to estimate the energy efficiency of TEMs.

During the design of engineering applications and development and testing of electrical and electronic components, circuits and systems, engineers try to find errors and obtain solutions in a shorter time by using measurement systems. Therefore, in order to achieve the correct solution, it is useful to know the properties of a material such as conductivity, permittivity and refractive indices to be used in circuits and systems. Thus, the determination stage of

(Received January 28, 2019; accepted June 18, 2019; published online June 25, 2019)

Table I. Parameters of the materials used for TE modules

Symbol	Name	σ (S/m and 10^6/cm Ω)		ε_r (@MW/IF)	δ (μm @1 MHz)
p-type					
Ca	Calcium	2.9×10^7	0.298	3 to − 22	93
Co	Cobalt	1.7×10^7	0.172	>100 to − 92	121
Ag	Silver	6.2×10^7	0.63	2.5 to − 55	63
Y	Yttrium	1.8×10^6	0.0166	N/A–N/A	384
La	Lanthanum	1.6×10^6	0.0126	(27)–N/A	447
Ce	Cerium	1.4×10^6	0.0115	(26) to − 0.3	453
Pr	Praseodymium	1.4×10^6	0.0148	(30)–0.08	412
Nd	Neodymium	1.6×10^6	0.0157	(10.5)–N/A	386
Sm	Samarium	1.1×10^6	0.00956	(13.5)–N/A	500
Eu	Europium	1.1×10^6	0.0112	(14)–0.13	474
Gd	Gadolinium	7.7×10^5	0.00736	(15)–N/A	582
Tb	Terbium	8.3×10^5	0.00889	(14)–N/A	530
Dy	Dysprosium	1.1×10^6	0.0108	(12)–N/A	477
Ho	Holmium	1.1×10^6	0.0124	(13) to − 1.5	443
Er	Erbium	1.2×10^6	0.0117	(14) to − 1.6	450
Yb	Ytterbium	3.6×10^6	0.0351	(15) to − 0.04	258
Lu	Lutetium	1.8×10^6	0.0185	(12) to − 8.5	366
n-type					
Zn	Zinc	1.7×10^7	0.166	(10.2) to − 68	120
Al	Aluminum	3.8×10^7	0.377	1.8 (10) to − 80	82
Ga	Gallium	7.1×10^6	0.0678	16.2–N/A	194
In	Indium	1.2×10^7	0.116	(9) to − 55	198
Ge	Germanium	2.1×10^3	1.45×10^{-8}	15.8–21	34

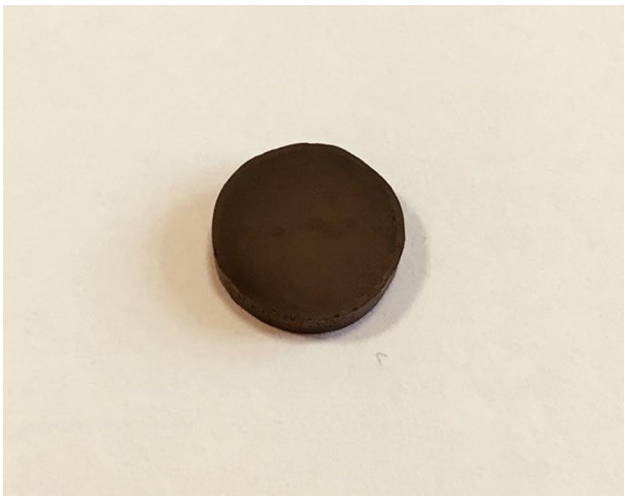

Fig. 1. Fabricated bulk sample.

appropriate material is performed in a shorter time with less cost and lower material and energy consumption levels without the need for the trial-and-error method.[9] Afterwards, the production stage of TEGs is started with the materials that are determined.

Dielectric properties are related to material structures, so they are determined by the material's molecular structure.[10] This way, all parameters of a material can be correlated as in dielectric properties. The factors that affect electrical conductivity and permittivity are density, structure, moisture, porosity, water content, frequency and temperature.[11,12] Therefore, these factors should be considered while designing electricity generating devices using semiconductor materials. Thus, a special study area such as material analysis may be developed by using the properties (electrical conductivity, permittivity and skin depth) of a material.

Complex permittivity and electrical conductivity are related to energy band structures. Permittivity is one of the most important parameters affecting the characteristic structures of semiconductor devices. Experimental results show that both the real and imaginary parts of this value depend on frequency and temperature of semiconductors.[13] The variation on free-carrier concentration, which affects conductivity, depends on the applied electric field or effects in temperature changes.[14] The conductivity associated with carriers of free-charge for doped semiconductors (with smaller energy gaps < 1 eV) is related to the activation energy of dopants.[15]

The relationship of electrical conductivity in semiconductors to other parameters was discussed, and the dependence of electrical conductivity on frequency and temperature was shown by experimental results. It was found that the dependence of electrical conductivity on frequency became weaker when temperature increased.[16] Since it is necessary to know the electrical conductivity value to understand the electron transport properties in semiconductors and have information about other parameters, electrical conductivity of a

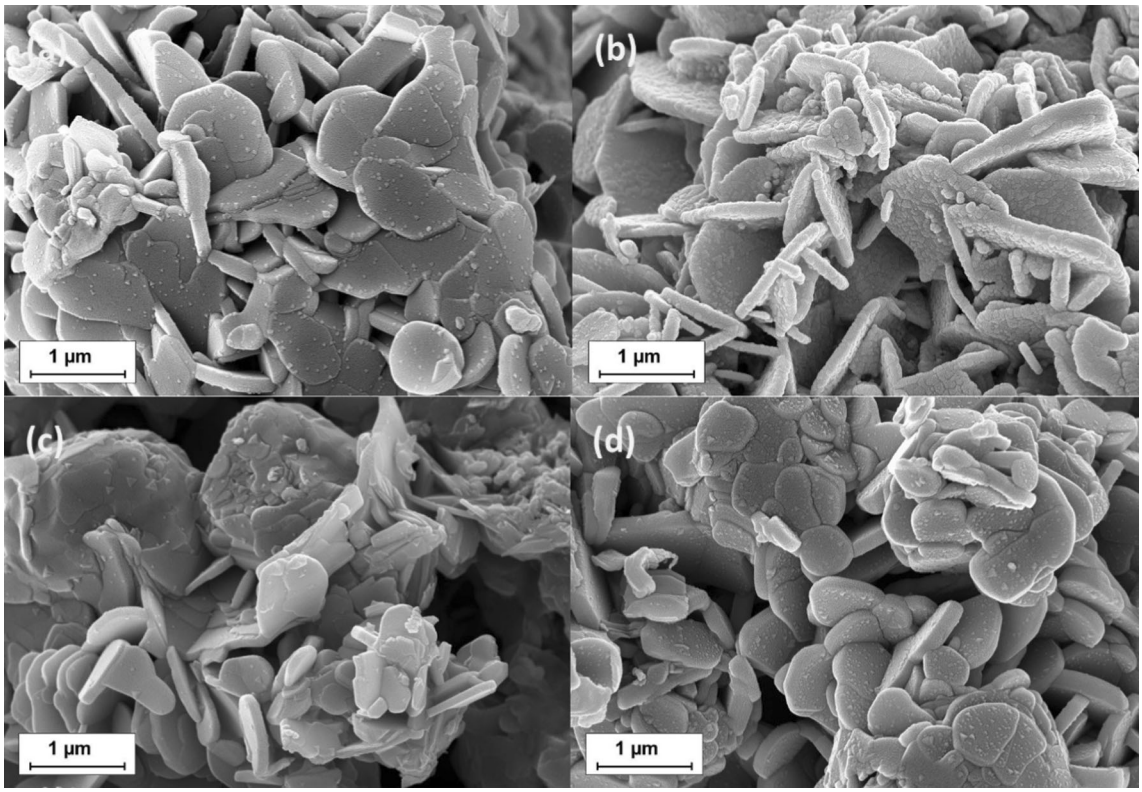

Fig. 2. SEM images of $Ca_{2.5}Ag_{0.3}RE_{0.2}Co_4O_9$ with × 50,000 magnification, *RE*: (a) Sm, (b) Yb, (c) Eu, and (d) Dy.

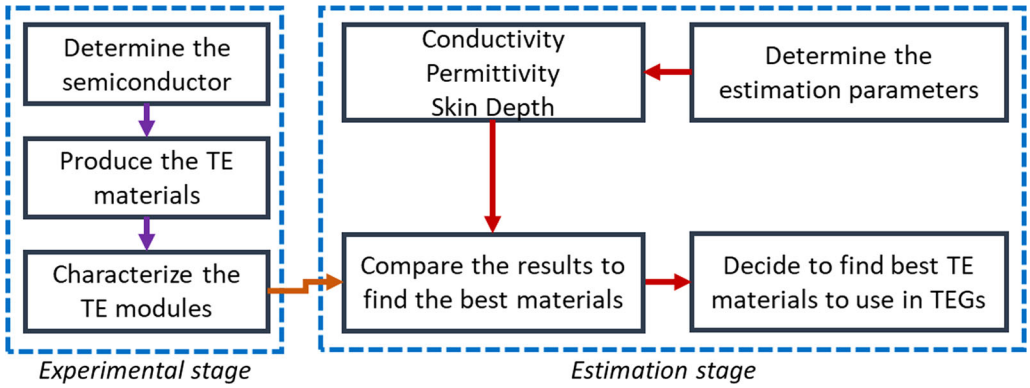

Fig. 3. Flowchart of the proposed model to present the steps.

semiconductor may be estimated using Drude theory.[17] Since the permittivity value is based on electrical conductivity, it will be affected by changes in conductivity. The electrical conductivity value is also affected by the carriers (electrons and holes) in semiconductor materials. Therefore, a relationship may be established between the permittivity value and the carriers. Thus, the change in permittivity may be monitored by controlling the carriers or carrier mobility.[13,18]

As an alternative, a parameter that affects temperature is skin depth. The penetration depth of a semiconductor material exposed to electromagnetic radiation is of fundamental importance.[19] The skin depth decreases when the electrical conductivity of a material increases since skin depth is inversely proportional to conductivity.[20] The penetration depth in semiconductors is found essentially independently from its amplitude at the surface. However, this parameter is determined by the characteristics of semiconductors.[19] In other words, the isothermal effect is related to skin depth intensity.[21] Although the skin depth parameter is associated with temperature, it becomes independent of temperature at very high frequencies. Therefore, the skin depth factor may be ignored at very high frequencies.[22] Although skin depth is mostly related to electromagnetic radiation, it is

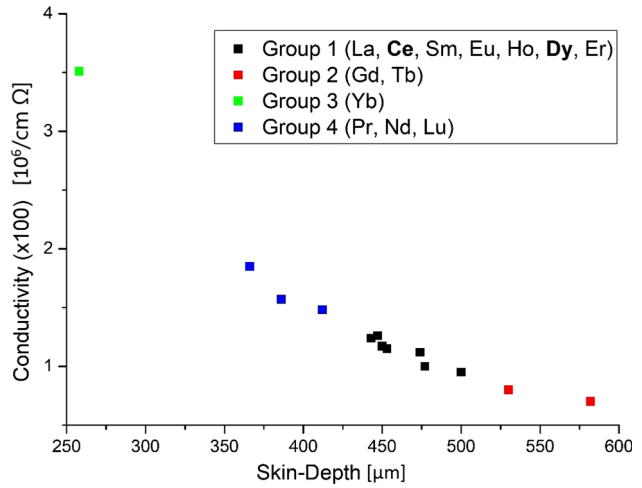

Fig. 4. Comparison of the electrical conductivity and skin depth parameters for lanthanide elements.

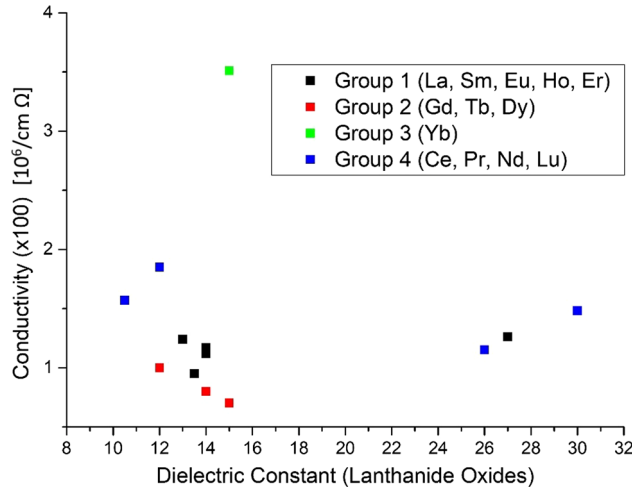

Fig. 5. Comparison of the electrical conductivity and dielectric constant parameters.

considered to be an effective parameter in obtaining preliminary information about the capacity of semiconductors to generate energy, which constitutes the focus in this study.

The most important goal here is to establish a relationship between the capacity to produce energy and the parameters (permittivity, conductivity, and skin depth) of a semiconductor material to be determined. The behavior of a TEM is estimated based on the predicted findings using electrical properties to decrease the cost of production. For this purpose, a model was developed to predict test results and reduce cost and process time. Thus, it was shown that thermoelectric modules could be considered in terms of energy efficiency to generate cost-effective TEMs and electricity in a short time. Consequently, new TEMs may be produced using the estimation values obtained from the proposed model in this study.

MATERIALS AND METHOD

When semiconductors are doped with other elements and heated, they can become efficient materials to fabricate thermoelectric modules and generate electricity. Firstly, the parameters representing the determinative properties of a semiconductor were discussed, and the production process of TEMs was then designed to form TEGs.

Electrical Properties of Semiconductors

The parameters of permittivity, permeability and electrical conductivity are commonly known as the electromagnetic properties of a material. When electromagnetic radiation passes through a material, two situations can occur due to the interaction between the material and the radiation: a part of the energy is stored in the material, and another part is lost from the electric field. Basically, the real part of complex permittivity represents the distinctive property for each material that maintains separated charges. On the other hand, the imaginary part of complex permittivity indicates the distinctive property for each material that allows charges to move.[23,24]

The complex permittivity in semiconductors is caused by electron transition (from valance band to conduction band) or electronic polarization.[25] Generally, the permittivity of a semiconductor is given as in Eq. 1,[15]

$$\varepsilon = \varepsilon_0\left(\varepsilon_r - j\varepsilon_r'' - j\frac{\sigma}{\omega\varepsilon_0}\right) = \varepsilon_0\varepsilon_r(1 - j\tan\delta) \quad (1)$$

where ε_0 is the permittivity value in free space, ε_r is the real permittivity value of a semiconductor, σ is the conductivity, and ω is the angular frequency. However, $\tan\delta$ may be described as the effective loss tangent of a material as given in Eq. 2:

$$\tan\delta = \tan\delta_d + \frac{\sigma}{\omega\varepsilon_0\varepsilon_r} \quad (2)$$

Here $\tan\delta_d$ is described as the loss tangent dependent on pure mechanisms (electronic and ionic polarization, etc.) of the semiconductor.

Electrical conductivity is crucial to measure the material's capacity to conduct electric current. This parameter (represented by sigma-σ and measured by Siemens per meter, S m^{-1}) may be described as the movement of charged particles. In this context, the resistivity of semiconductors may be changed by an externally applied electric field. The effect of electrical conductivity may be ignored at high frequencies since its value is inversely proportional to frequency. While this approach is applicable to non-conductive materials, there is an exceptional case for metals. The relationship between electrical conductivity and the temperature in a semiconductor material is described as an increasing conductivity when temperature is increased. Thus, the temperature will cause an

Table II. Determination of zT values for TEMs at different temperatures

No.	Composition	Temperature (°C)						
		200	300	400	500	600	700	800
p-type								
1	$Ca_{2.5}Ag_{0.3}Nd_{0.2}Co_4O_9$	0.18	0.23	0.29	0.34	0.39	0.42	0.52
2	$Ca_{2.5}Ag_{0.3}Sm_{0.2}Co_4O_9$	0.17	0.24	0.31	0.36	0.43	0.54	0.51
3	$Ca_{2.5}Ag_{0.3}Er_{0.2}Co_4O_9$	N/A	0.19	0.24	0.30	0.36	0.41	0.54
4	$Ca_{2.5}Ag_{0.3}Yb_{0.2}Co_4O_9$	0.01	0.17	0.32	0.37	0.38	0.43	0.47
5	$Ca_{2.5}Ag_{0.3}Eu_{0.2}Co_4O_9$	0.15	0.19	0.27	0.35	0.45	0.49	0.57
6	$Ca_{2.5}Ag_{0.3}Lu_{0.2}Co_4O_9$	0.15	0.22	0.29	0.35	0.41	0.48	0.50
n-type								
1	$Zn_{0.96}Al_{0.02}Ge_{0.02}O$	0.02	0.04	0.01	0.01	0.02	0.03	0.04
2	$Zn_{0.96}Al_{0.02}Ga_{0.02}O$	0.02	0.03	0.05	0.07	0.10	0.13	0.17
3	$Zn_{0.96}Al_{0.02}In_{0.02}O$	0.01	0.02	0.03	0.04	0.06	0.09	0.12

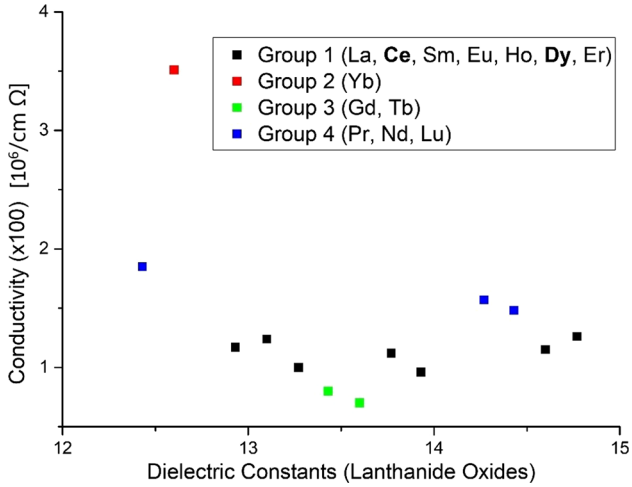

Fig. 6. Comparison of the electrical conductivity and dielectric constant parameters.

increase in the conductivity of a semiconductor by an increase in the density of charge carriers. On the other hand, in a high temperature regime for semiconductors, electrical conductivity will increase depending on electron concentration.[26–28]

Two factors, free-carriers concentration and mobility, affect the electrical conductivity of a material. Importantly, both carrier concentration and mobility are temperature-dependent. Furthermore, electrical conductivity is dependent on the band gap of a semiconductor and temperature. Total electrical conductivity in intrinsic semiconductors may be described as the sum of conductivities of the conduction and valance band carriers which are electrons and holes. In this context, the electrical conductivity in intrinsic semiconductors is stated as given in Eq. 3,[26–28]

$$\sigma = n_e q_e \mu_e + n_h q_h \mu_h \tag{3}$$

where μ is the mobility, q is the charge, and n is the concentration. Additionally, e and h are used to denote the electrons and holes, respectively. Moreover, electrical conductivity may be expressed as a function of temperature as in Eq. 4,[29]

$$\sigma = \sigma_o \exp\left(\frac{-\Delta E}{k_B T}\right) \tag{4}$$

where σ_o is the constant of the pre-exponential, ΔE is the thermal activation energy of conductivity, k_B is the Boltzman constant, and T is the temperature. In a different way, electrical conductivity may be defined as in Eq. 5:

$$I = \frac{\sigma V A}{L} \tag{5}$$

Here A is the cross-sectional area, L is the length, V is the applied voltage, and I is the electric current. As an alternative to the formulae given above, it is possible to reach different versions of permittivity and electrical conductivity formulae. However, in general, these formulae are used to describe the electrical conductivity and permittivity parameters.

The skin depth (effect) in materials is an important parameter for lower frequencies. However, this parameter is neglected for frequency ranges of microwave and millimeter waves, since the electromagnetic field does not penetrate inside a material bigger than a micrometer. Therefore, skin depth is related to the frequency band, as well as the material's type and geometry. Furthermore, it is directly proportional to the material's resistivity. Therefore, the resistivity of a material increases when skin depth decreases. However, an increase in resistivity is not desirable for TEMs. Moreover, the power capacity of a material decreases with a decrease in skin depth. On the contrary, power concentration on the surface increases with decreasing skin depth. Nevertheless, the skin-depth theory is related to Maxwell's equations for isotropic media. Skin depth is usually defined as in Eq. 6:[21]

$$\delta = 1/\sqrt{\pi f \mu \sigma(T_s)} \tag{6}$$

Here f is the frequency, μ is the magnetic permeability, σ is the electrical conductivity of a semiconductor, and T_s is described as the surface temperature of the semiconductor. As seen in Eq. 6, skin depth decreases when frequency increases.

The rounding values of the parameters that were used in this study are given in Table I. The real part of the permittivity (relative permittivity or dielectric constant) values of each element could not be found (not available, N/A) in the literature. Therefore, the values of these parameters were added partially and were collected at around a 300 K. Before the slash sign in the permittivity column, the values in the microwave (mw) frequency range are presented. The values that are presented in brackets of lanthanide elements are for oxide structures. In the same column after the slash sign, the negative (or positive) values of the dielectric constant parameter between 200 nm and 1000 nm of wavelength range (infrared, IR) are added to demonstrate different approaches for estimating a model, since the dielectric constant values of metals depend on external electromagnetic fields.[30–39] When frequency increases, this parameter may become negative. In other words, electromagnetic radiation is reflected by metals. When frequency increases even higher, the dielectric constant parameter becomes positive. Moreover, it should be noted that the relative permittivity of all metals at low frequencies (kHz or MHz) is around 1.

Fabrication and Characterization of TEMs

A semiconductor, which has two bands (valance and conduction bands with a forbidden gap), is a material that has an electrical conductivity between those of a conductor and an insulator. It needs external energy (e.g. in heat form) to move the electrons from the valance band to the conduction band.[6] When TEMs are connected electrically in series and thermally in parallel, the charge carriers (electrons and holes) diffuse from the hot side to the cold side of a TEG to compose an effective voltage. To date, oxide TEMs have attracted great attention since they have low toxicity and are chemically stable in air at high temperatures.[6,7]

There are some methods to produce bulk TEMs such as cold pressing (CP), spark plasma sintering (SPS), solution combustion (SC) and hot pressing (HP) after obtaining a powder form by the solid-state reaction, sol–gel, self-ignition, polyacrylamide gel and wet chemical methods.[6,7] Co complexes (due to higher crystallinity) have been found to show higher conductivity than Ni complexes.[29] Because of these characteristics, oxide TEMs are expected to have good energy efficiency. To demonstrate the predictive ability of the proposed method, p- and n-type TEMs were produced using the sol–gel method. Nitrate salts of the specified elements were used in stoichiometric ratios as the starting materials. Distilled water was used as the solvent to dissolve each precursor to be fully dispersed and form homogenous solutions. After dispersion of the precursors, the solutions were mixed and magnetically stirred at 100°C to obtain the final homogeneous solutions. Xerogel formation was achieved by adding citric acid monohydrate into the solutions as the chelating agent. After gelation, the obtained xerogel was dried at 200°C for 2 h to remove moisture and undesired gases. Before x-ray diffraction (XRD) analysis, the dried powders were calcined at 800°C for 2 h to obtain target phases. The XRD patterns of the final powders were identified by a Thermo Scientific ARL model x-ray diffractometer using Cu K_α irradiation (wavelength, λ = 1.540562 Å) in the range of $5° \le 2\theta \le 90°$ at a speed of 2°/min.

The pre-shaped samples were consolidated by CP at 1100 MPa. As the next step, the samples were subjected to heat treatment for 24 h at 900°C to obtain consolidated bulk samples (Fig. 1). The surface morphologies and microstructures of the bulk samples were observed by a Zeiss Ultra Plus Gemini model scanning electron microscope (SEM). The thermopower and electrical resistivity of the samples were measured by a Linseis LSR-3 system. The thermal conductivity values of the materials were calculated using Eq. 7,

$$\kappa = \alpha \rho c_p \tag{7}$$

where κ is the thermal conductivity, α is the thermal diffusivity, ρ is the density, and c_p is the specific heat capacity of TEMs.[6] The thermal diffusivity values of the bulk samples were measured by a Netzsch LFA 457 MicroFlash Apparatus *via* the laser flash method. The specific heat capacities of the samples were determined by using the law of Dulong and Petit, and the densities of the bulk samples were measured using Archimedes' principle. The figure of merit (zT) values, which are efficiency expressions of TEMs, were calculated by

$$zT = \frac{\alpha^2 T}{\rho \kappa} \tag{8}$$

where α is the thermopower, ρ is the electrical resistivity, T is the absolute temperature, and κ is the total thermal conductivity.[6]

The SEM micrographs of the $Ca_{2.5}Ag_{0.3}RE_{0.2}Co_4O_9$ (*RE*: Sm, Yb, Eu and Dy) samples are given in Fig. 2, revealing that the samples were in a plate-like structure exhibiting a layered crystal structure in accordance with the crystal structure of $Ca_3Co_4O_9$. $Ca_{2.5}Ag_{0.3}RE_{0.2}Co_4O_9$ particles were intergrown, so that clear boundaries were not observed. Additionally, the bulk samples had porous structures indicating lower experimental densities of 3.80 g/cm^3 on average with a relative density of 81%. According to the SEM images, these results were in accordance with the particle size distribution, surface area and unapparent grain boundaries.

In fact, 17 compositions were fabricated during the experiments, but analysis results of nine compositions were added to Table II. As seen in Table - II, the elements Ca, Ag, Co and O were common for *p*-type compositions. Likewise, Zn, Al, and O were common for *n*-type compositions. Therefore, the proposed model would be composed of and compared using rare-earth elements (lanthanide group).

In addition to Table II, the values of the generated energy were measured at 700°C and 800°C, respectively, for La (0.47 and 0.48), Pr (0.34 and 0.58), Gd (0.33 and 0.19), Dy (0.22 and 0.25), Tb (0.27 and N/A), Ho (0.50 and N/A), Ce (0.21 and 0.21) and Y (0.34 and 0.17).

Characterization of the produced materials was carried out to verify proper doping with formation of target phases. Dual-doped samples were investigated based on their thermopower values to be used at high temperature applications. It was determined that the thermopower of the samples decreased by increasing electron concentration due to the doping process.

The experimental results were used to demonstrate the predictive capability of the proposed model. In order to show the determinative properties of the selected parameters, the characterization results of the produced TEMs were compared to values found in the literature as supporting findings. The first part consisted of experimental stages, while the second part showed the working principle of the proposed model. To summarize the proposed model, a flowchart was prepared as shown in Fig. 3.

The k-means technique is commonly used for clustering problems and very popular for data clustering. It divides a composed data set into k-groups. This process continues by choosing the initial cluster (k) centers. The cluster number should be determined by the user before analyzing the data set. The Euclidean squared distance is simply used by this algorithm. The goal of the algorithm is to minimize the distribution within the cluster to perform the best classification.[24,40] Thus, the relevant materials in the data set may be identified based on their common characteristics. Additionally, an easy to use k-means algorithm is available in many program packages.

RESULTS AND DISCUSSION

It was found in previous studies that electrical conductivity and permittivity are temperature-dependent. We focused on the approach that TEGs are a kind of application where the electrical and thermal properties of semiconductor materials are used. When the data given in Tables I and II are examined, it may be seen that a relationship between electrical conductivity and skin depth could be established. According to the theoretical information, electrical conductivity is expected to increase while the value of skin depth decreases before the production process of TEMs. However, the skin depth value should increase since the resistivity parameter is the inverse of conductivity. Furthermore, the power capacity of the material will increase as the skin depth of it increases depending on conductivity. Thus, independent from the thermal properties, a comparison may be made between the components of TEMs and the conductivity parameter.

In each composition, instead of the elements used as common (Ca, Co and Ag), doped elements (lanthanide group for *p*-types) were also considered. The reason was that the dielectric constant of the $Ca_3Co_4O_9$ structure was considered as a giant value of 1.38×10^4 (at 1 kHz).[36] Furthermore, the goal of the study was to investigate the effects of different doping materials. Moreover, the conductivity values of the elements Ca, Ag and Co are higher than the others. However, the skin depth values were lower for these elements. Anyway, the electrical conductivity value was more important than the skin depth value.

As seen in Table II, the best doped materials were expected to be Eu, Sm, Yb and Er. There was a compatibility between the electrical conductivity and skin depth parameters of these four elements in the lanthanide group. When skin depth increased, they would have higher conductivity. However, the presence of a few elements in the same situation makes it difficult to determine which element is better. Therefore, it is expected that the materials will be classified in relation to their properties by the well-known method of k-means. In this context, the classification process was applied for 13 different lanthanide elements except Y. First of all, it was possible to classify the elements that were the most similar to each other using the electrical conductivity and skin depth parameters, and the results are shown in Fig. 4. The y-axis of the plot was revised by multiplication by 100 for visualization.

As shown in Fig. 4, all groups were automatically generated by the k-means algorithm. As only two parameters were compared at this stage, the presence of the Ce and Dy elements in Group 1 (black) as an unexpected situation made the proposed method unsuccessful. On the other hand, when we refer to Group 1, it is understood that Group 2 (red) formed by the Gd and Tb elements should not be preferred. It also appears that Group 4 (blue) may be used in TEM compositions as an alternative to Group 1 (black). This situation was also confirmed by the values shown in Table II. The reason why Group 3 (green) was out of place was that its electrical conductivity was higher than those of the other elements. The reason for not being included in Group 1 (black) was the low skin depth value of it (Yb).

In order to eliminate the negative situation caused by the co-evaluation of the two parameters, the real part of permittivity given in Table I was included in the k-means algorithm as a new variable. The results that were obtained are given in

Fig. 5. The data in brackets (before the slash sign) given in Table II were used to illustrate the effects of the oxide states of the preferred materials.

With the effect of the new parameter (dielectric constant), the Ce and Dy elements in Group 1 (black) emerged in different groups. The emergence of Dy in Group 2 (red) in accordance with the result shown in Table II showed the success of the newly added parameter. However, since the element Ce was found in Group 4 (blue), which was an alternative to Group 1 (black), this suggested that the proposed model should be supported by a new variable. When different values of the dielectric constant were used for the classification process the by k-means algorithm, the results shown in Fig. 6 were similar to those shown in Fig. 4 (based on skin depth). The values that were used for this step (Fig. 6) were sorted as La 14.77, Ce 14.6, Pr 14.43, Nd 14.27, Sm 13.93, Eu 13.77, Gd 13.6, Tb 13.43, Dy 13.27, Ho 13.1, Er 12.93, Yb 12.6 and Lu 12.43.[37,38]

As seen in Fig. 6, the success of the proposed model was moderate. Therefore, either a new parameter must have been added, or the literature values should have been determined as the most accurate ones. For this purpose, it was necessary to accurately determine the properties of the materials using the measurement methods of microwave measurement or Terahertz-Time Domain Spectroscopy/THz-TDS systems. Furthermore, it was not possible to create a data set, which would require the use of the k-means algorithm, since the *n*-type TEMs were produced with three different elements.

Since the preferred parameters in the proposed model were frequency-dependent, the frequency range of the application was important. Therefore, it was crucial to measure each material to be preferred with the appropriate spectroscopy method (microwave, millimeter wave or THz frequency range) in the corresponding frequency range. When these parameters are measured or obtained correctly, they can provide valuable information for engineers and scientists to properly use semiconductors for TE modules in their design and production processes. Although the real part of the complex permittivity values given in Table I had different values at different frequencies, this is affected by the materials with the best results with regards to the selected frequency region. Thus, knowing the properties of materials would provide an estimation of how much energy capacity will be generated by the TEGs to be produced. On the other hand, doping amounts affect the permittivity and electrical conductivity values of compounds.

In the proposed model, the preferred parameters were evaluated independently and compared to the experimental results. These parameters, which were selected for the characteristics in this study, enabled the recognition and use of a semiconductor material. Simulation results were aimed to be associated with temperature increase, which is the working principle of TEGs. Although the temperature and frequency changes affected permittivity and conductivity, the values of these parameters were compiled at a constant temperature (nearly at 300 K), and the measurement results were supported by the simulation results.

When the simulation and experimental results were evaluated together, it was shown that the compound, which was intended to be formed before producing a new TEG, could be found to be highly efficient or not. However, the importance of thermopower should not be forgotten. The parameters that were used in this study were evaluated independently from the thermopower, and the significance of the selected parameters was revealed by using the experimental results.

CONCLUSION

Unlike conventional energy generating devices, TEMs may be connected to each other without any moving parts. Before the production of new TEMs, the proposed model for predicting which semiconductor material could increase energy efficiency was supported by the experimental results. Using electrical properties without accounting for the effects of temperature, an estimated approach for the energy generation capacity of TEGs was demonstrated. It was stated that the permittivity, conductivity and skin depth characteristics of semiconductors may be useful before proceeding with the production and testing steps, which are expensive processes. Thus, the energy efficiencies of the *p*- and *n*-type TEMs were shown and supported by the experimental results. Accordingly, thanks to the proposed method, the workforce and cost would be significantly reduced, and time would be saved. Therefore, before designing a TEM, the electrical and optical properties of conductive and semi-conductive elements must be examined, and the materials to be used should be determined. Therefore, the measurement process should be performed with a THz-TDS system in a wide frequency range, and the characteristics of each material should be discussed. Thus, it will be easier to access the missing information in the literature. Additionally, if the material is measured in the THz frequency region, the proposed method can be applied for other material systems, because it is possible to determine the relevant parameters of the materials as a distinct fingerprint in the specified frequency region.

REFERENCES

1. E. Kayabasi, M.A. Alperen, and H. Kurt, *Int. J. Green Energy* 16, 200 (2019).
2. E. Kayabasi and H. Kurt, *Eng. Sci. Technol. Int. J.* 21, 70 (2018).
3. F.B. Özkul, E. Kayabasi, E. Çelik, H. Kurt, and E. Arcaklioğlu, in *2018 International Conference on Photovoltaic Science and Technology* (IEEE Explore Digital Library, 2018), pp. 1–6.

4. M. Yilmaz, E. Kayabasi, and M. Akbaba, *Eng. Sci. Technol. Int. J.* (2019). https://doi.org/10.1016/j.jestch.2019.02.006; https://www.sciencedirect.com/science/article/pii/S2215098618321803. Accessed 22 June 2019.
5. F. Zhang, B. Niu, K. Zhang, X. Zhang, Q. Lu, and J. Zhang, *J. Rare Earths* 31, 885 (2013).
6. E. Kilinc, S. Demirci, F. Uysal, E. Celik, and H. Kurt, *J. Mater. Sci. Mater. Electron.* 28, 11769 (2017).
7. F. Uysal, E. Kilinc, H. Kurt, E. Celik, M. Dugenci, and S. Sagiroglu, *J. Electron. Mater.* 46, 4931 (2017).
8. C. Baker, P. Vuppuluri, L. Shi, and M. Hall, *J. Electron. Mater.* 41, 1290 (2012).
9. T. Ozturk, O. Morikawa, İ. Ünal, İ. Uluer, and J. Infrared, *J. Infrared Millim. Terahertz Waves* 38, 1241 (2017).
10. T. Ozturk, M. Hudlička, and İ. Uluer, *J. Infrared Millim. Terahertz Waves* 38, 1510 (2017).
11. S. Latkowski, J. Parra-Cetina, R. Maldonado-Basilio, P. Landais, G. Ducournau, A. Beck, E. Peytavit, T. Akalin, and J.F. Lampin, *Appl. Phys. Lett.* 96, 23 (2010).
12. H. Treichel, *J. Electron. Mater.* 30, 290 (2001).
13. Y. Li, P. Su, S. Gao, Q. Shen, and M. Gong, *Microelectron. Eng.* 159, 143 (2016).
14. T.O. Gegechkori, V.G. Yakeli, and Z.S. Kachlishvili, *Phys. Status Solidi* 112, 379 (1982).
15. J. Krupka, J. Breeze, A. Centeno, N. Alford, T. Claussen, L. Jensen, and I.E.E.E. Trans, *Microw. Theory Tech.* 54, 3995 (2006).
16. B.V. Klimkovich, N.A. Poklonski, and V.F. Stelmakh, *Phys. Status Solidi* 134, 763 (1986).
17. E.A. Bondar, S.A. Gormin, I.V. Petrochenko, and L.P. Shadrina, *Opt. Spectrosc.* 89, 892 (2000).
18. K. Alfaramawi, *Open Phys.* 13, 334 (2015).
19. O.A. Kosygin, V.N. Chupis, and A.Y. Somov, *Tech. Phys.* 44, 602 (1999).
20. Y. Iwashita, in *22nd International Linear Accelerator Conference* (2004), pp. 700–702.
21. Z. Nie, Y. Hou, J. Deng, P.A. Ramachandran, S. Wen, and W. Ma, *Appl. Therm. Eng.* 125, 856 (2017).
22. A. Ayachit and M.K. Kazimierczuk, *IEEE Magn. Lett.* 4, 0500304 (2013).
23. T. Ozturk, *J. Nondestruct. Eval.* 38, 11 (2019).
24. T. Ozturk, *J. Hazard. Mater.* 363, 309 (2019).
25. M. Li and H. Li, *IEEE Trans. Nanotechnol.* 11, 1004 (2012).
26. H. Ibach and H. Lüth, *Solid-State Physics* (Berlin: Springer, 2009).
27. A. Sconza and G. Torzo, *Eur. J. Phys.* 10, 123 (1989).
28. S. Kasap, *Principles of Electronic Materials and Devices* (New York: McGraw-Hill, 2005).
29. S.M. Morgan, N.A. El-Ghamaz, and M.A. Diab, *J. Mol. Struct.* 1160, 227 (2018).
30. G. Kian Heng, Samarium Oxide and Samarium Oxynitride Thin Film Gate Oxides on Silicon Substrate Thesis Submitted in Fulfillment of the Requirements for the Degree of Doctor of Philosophy Faculty of Engineering University of Malaya Kuala Lumpur 2017, University of Malaya (2017).
31. K.C. Chang, Y.C. Yeh, and J.T. Lue, *Meas. J. Int. Meas. Confed.* 45, 808 (2012).
32. A. Paskaleva, D. Spassov, and P. Terziyska, *J. Phys. Conf. Ser.* 794, 012017 (2017).
33. K.F. Young and H.P.R. Frederikse, *J. Phys. Chem. Ref. Data* 2, 313 (1973).
34. M. Fernández-Perea, J.I. Larruquert, J.A. Aznárez, J.A. Méndez, L. Poletto, D. Garoli, A.M. Malvezzi, A. Giglia, and S. Nannarone, *J. Opt. Soc. Am. A* 24, 3691 (2007).
35. J.I. Larruquert, A.P. Pérez-Marín, S. García-Cortés, L. Rodríguez-de Marcos, J.A. Aznárez, and J.A. Méndez, *J. Opt. Soc. Am. A* 28, 2340 (2011).
36. N. Prasoetsopha, S. Pinitsoontorn, P. Thongbai, and T. Yamwong, *Electron. Mater. Lett.* 9, 347 (2013).
37. D. Xue, K. Betzler, and H. Hesse, *J. Phys. Condens. Matter* 12, 3113 (2000).
38. J.St. Jur, Lanthanide-Based Oxides and Silicates for High-K Gate Dielectric Applications, North Carolina State University (2007).
39. V. Palenskis, *World J. Condens. Matter Phys.* 03, 73 (2013).
40. T. Ozturk, *Sak. Univ. J. Sci.* 23, 724 (2019).